

Dust formation in the Cassiopeia A supernova^{*}

P.O. Lagage¹, A. Claret¹, J. Ballet¹, F. Boulanger², C.J. Césarsky¹, D. Césarsky², C. Fransson³, and A. Pollock⁴

¹ CEA/DSM/DAPNIA/Service d'Astrophysique, CE Saclay F-91191 Gif-sur-Yvette, France

² Institut d'Astrophysique Spatiale, Université d'Orsay, F-91405 Orsay, France

³ Stockholm Observatory, S-13336 Saltsjöbaden, Sweden

⁴ ISO SOC, European Space Agency, P.O. Box 50727, Madrid, Spain

Received 16 July 1996 / Accepted 6 August 1996

Abstract. High angular resolution (6") spectro-imaging observations of Cassiopeia A, the youngest supernova remnant of our galaxy, were performed with ISOCAM, the mid-infrared camera on board of the Infrared Space Observatory (ISO). The remnant was fully mapped with the LW8 filter (10.7–12 μ m), which probes mainly dust thermal emission. Emission is seen both from the blast wave region and the inner region; the north-eastern jet region outside the nominal radius of the remnant is also detected. Additional spectro-imaging observations of the northern part of the remnant were done in order to better characterise the dust and its link to the gas. The gaseous ionic emission lines of sulphur (SIV at 10.5 μ m) and of neon (NeII at 12.8 μ m) were observed with the ISOCAM Circular Variable Filter at a spectral resolution of 40. The gas emission is spatially well correlated with the so-called fast moving knots seen in the optical and which are known to be made of nuclear burning products from the progenitor star. The dust continuum was observed at 9.8, 11.3 and 12 μ m. The LW9 filter (14–16 μ m) was also used. A very good spatial correlation between gas and dust emission is revealed by the observations. This is a good hint that dust formation took place in the knots and that we are observing supernova grains in the evaporating interfaces between cool optical knots and the hot supernova cavity gas.

Key words: ISM: supernova remnants – supernovae individual: Cas A – dust – infrared: general

1. Introduction

The idea that part of the interstellar dust is formed from supernova ejecta material was proposed in order to explain isotopic composition anomalies found in meteorites (Clayton 1978,

Send offprint requests to: Lagage@sapvxa.saclay.cea.fr

^{*} Based on observations with ISO, an ESA project with instruments funded by ESA Member States (especially the PI countries: France, Germany, the Netherlands and the United Kingdom) and with the participation of ISAS and NASA.

Amari et al. 1992 for a more recent discussion). Strong indirect evidences that dust does form in supernovae (SN), arise from the observations of SN1987A (Lucy et al. 1989, Moseley et al. 1989, Bouchet et al. 1991, Suntzeff et al. 1991, Wooden et al. 1993, Colgan et al. 1994). Additional evidences can be gathered by mapping the InfraRed (IR) emission from supernova remnants. A very good candidate is Cassiopeia A, the youngest known supernova remnant of our galaxy, aged of about 343 years.

Infrared emission from Cas A has been observed with the IRAS satellite (Dwek et al. 1987, Braun 1987). The observed emission arises mainly from dust collisionally heated by the hot gas emitting X-rays. However, due to the limited angular resolution of the observations with IRAS (30"), it was not possible to assess whether the emission originates from interstellar dust heated by the hot gas associated to the forward shock or from circumstellar, SN condensates heated by the hot gas associated to the reverse shock or ... In this paper, we present mid-IR observations at high angular resolution (6") obtained with the ISOCAM camera (Césarsky et al. this issue) on board of ISO (Kessler et al. this issue). Section 2 deals with the observations of both the dust emission and the gas emission. In Sect. 3, we discuss the nature of the dust at the origin of the radiation observed in the mid-IR.

2. Observations and results

2.1. Mapping of the whole remnant

With ISOCAM, we were able to map the Cas A mid-IR emission with an angular resolution of 6". The LW8 filter (10.7–12 μ m) was chosen in order to probe mainly the dust emission; the main gaseous ionic lines are, either outside of the wavelength coverage of the filter (ArIII, NeII), or in the short wavelength wing of the filter (SIV). With the pixel field of view of 6", the camera is viewing a 3'x3' field (32x32 pixels). In order to image the whole remnant (about 4'x4') and to have access to the adjacent sky background, a raster map was performed. The raster was composed of 24 frames (6x4 frames along the x and y axis of the satellite). An overlap of half a frame from one frame

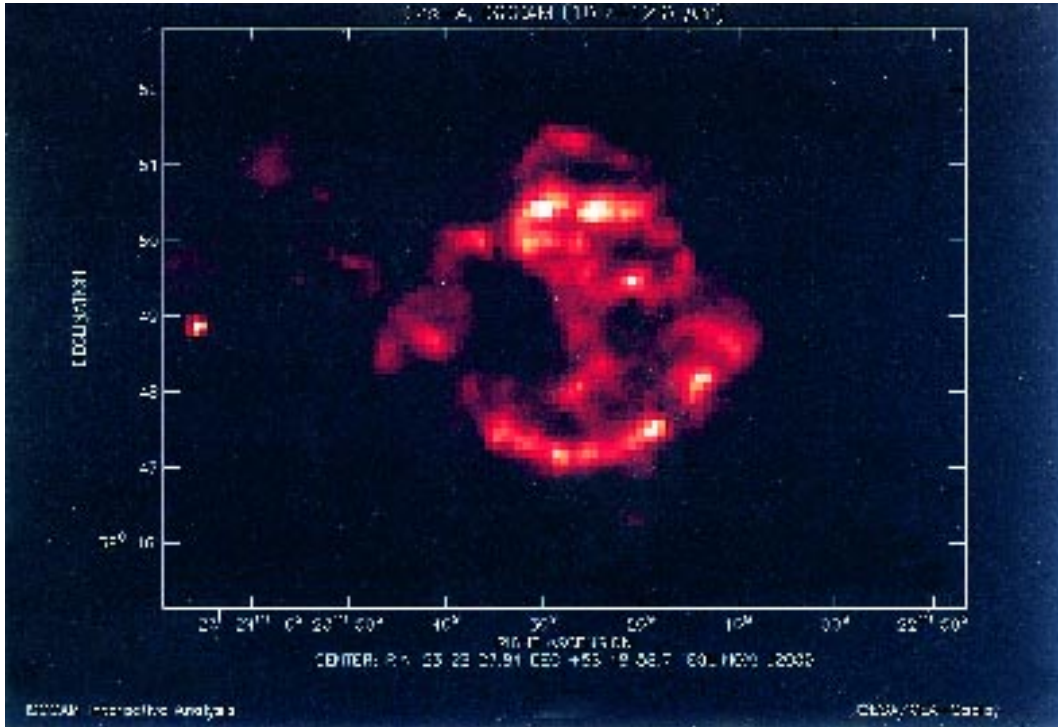


Fig. 1. Cas A as observed with the ISOCAM LW8 filter (10.7-12 μ m) at a spatial resolution of 6 arcsec.

to another was set, so that, in total, a 9'x6' field was covered. A total integration time of 53s was spent on each frame, (25 images with an elementary integration time of 2.1s).

Data reduction was performed with CIA¹ in four steps. First, the images were deglitched from the cosmic rays induced signal; the SAp (Service d'Astrophysique) multi resolution method was used (Starck et al. 1995). Second, the signal was corrected from detector memory effects; (the SAp transient fitting model was used). Third, the sky background contribution was removed using the frames free from SNR emission; (note that this subtraction also removes the detector dark current). The last step was to correct the image from the inhomogeneities of the detector response (flat-field); the flat-field correction factor was taken from the ISO calibration data base. The resulting image is shown on Fig. 1.

The total flux integrated over a circle with a 3' radius centered at R.A. (J2000) = 23^h 23^m 27.7^s, Decl. (J2000) = +58° 48' 58.5", is found to be 12.3 \pm 2.5 Jy. The calibration was done with the system response value given in the ISOCAM observer manual (0.726 ADU/s/mJy; ADU stands for Analog to Digital Unit). The uncertainties due to the data processing were estimated by using different methods of flat-field correction, transient correction, sky subtraction...; a conservative value of \pm 20% was set. The central value for the flux deduced here is lower than the central value found from IRAS measurements, 16.9 Jy (Dwek et al. 1987). But the IRAS filter was broad (8-15 μ m) and was encompassing gaseous line emission.

¹ CIA is a joint development by the ESA astrophysics division and the ISOCAM consortium led by the ISOCAM PI, C. Césarsky, Direction des Sciences de la Matière, C.E.A., France.

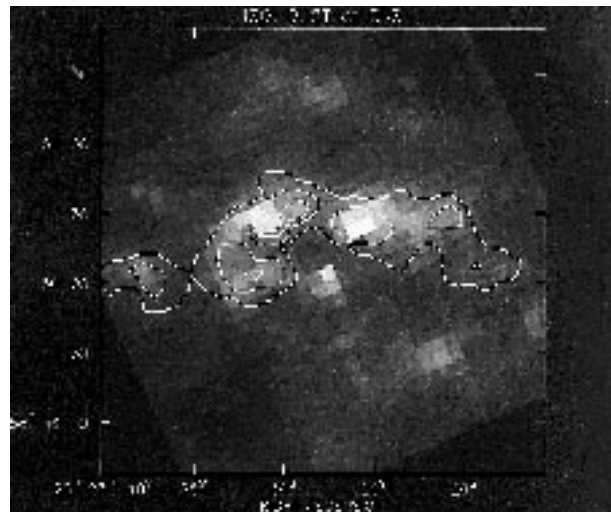


Fig. 2. Contour plot of the SIV line emission (the underlying continuum has been subtracted) overlaid over an image of the 11.3 μ m dust emission observed by ISOCAM. At each contour the flux level is divided by two.

The morphology of the emission at this angular resolution shows that there is a bright ring of emission at a radius of about 100". This radius is less than the blast wave radius of 140", as determined from X-ray observations (Murray et al. 1979, Fabian et al. 1980). Thus most of the emission does not originate from interstellar dust heated by the expanding supernova blast wave. Only the faint emission northern of the bright ring could be attributed to such dust, (but see Borkowski et al. 1996). Note

that IR emission is also observed outside the blast wave radius in the north-eastern region; this emission is coincident with the fastest moving knots seen in the optical (Fesen et al. 1988). The origin of the emission from the bright ring can be either dust heated by the hot gas in the reverse shock moving inward the remnant or circumstellar, SN condensates in the evaporating flow associated with the metal rich gaseous cool knots observed in the visible (van den Bergh & Kamper 1983, Reed et al. 1995)...

2.2. Spectro-imaging of the northern part

In order to ascertain the origin of the dust emission in the bright ring and its link with the gaseous component, we made spectro imaging observations with the Circular Variable Filter (CVF) of ISOCAM; the spectral resolution is 40. We restricted such observations to one frame ($3' \times 3'$) on the remnant and one frame on the background. We focused on the northern bright region. This region emits almost half of the total emission from the remnant. The on-source frame was centered at R.A. (J2000) = $23^h 23^{min} 27.7^s$, Decl. (J2000) = $+58^\circ 50' 13.5''$. Five CVF wavelengths were chosen; three wavelengths were probing the dust: $9.8\mu\text{m}$, $11.3\mu\text{m}$ and $12\mu\text{m}$; two wavelengths were probing the gas: $10.5\mu\text{m}$ (SIV) and $12.8\mu\text{m}$ (NeII). The total on-source integration time varied from 3 to 5 min according to the wavelength. The region was also observed with the LW9 filter ($14\text{--}16\mu\text{m}$) during 3 min. The data have been processed as described in Sect. 2.1.

Both the gas and dust are detected. The gas is detected both in the SIV line and the NeII line. SIV was already marginally detected in one optical knot from ground-based observations (Dinerstein et al. 1987), but it is the first detailed mapping in the line, as well as the first detection of NeII line. The SIV ionic line emission and the $11.3\mu\text{m}$ dust emission are shown on Fig. 2. The gaseous lines are not seen in the northernmost part of the remnant. The results of the photometry are shown on Fig. 3; the lines contribute at the level of 40% to the total flux in the range $9.8\text{--}12.8\mu\text{m}$.

3. Discussion

On Fig. 4, the spatial distribution of the SIV line has been compared with the spatial distribution of the SII lines observed in the visible. A very good correlation is found, so that the SIV has certainly the same origin as the SII lines, i.e. the shock heated gas in the so-called fast-moving knots (FMK's). These FMK's are made of nuclear products from the progenitor star (Lamb 1978; Chevalier & Kirshner 1979). Dust formation may have taken place in these gaseous knots. If such, then SN condensates should be found in the evaporating flow at the interface between the cool FMK's and the hot SN cavity gas. These grains are heated collisionally by the gas in the flow and radiate in the mid-IR (Dwek & Werner 1981). The good spatial correlation between gas and dust as shown on Fig. 2 is a strong case in favour of the previous scenario.

We have compared the spatial distribution of the dust emission and of the X-ray emission, which traces the gas which can

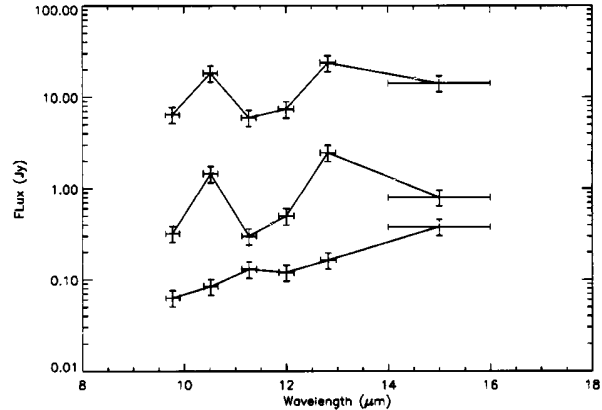


Fig. 3. Flux as a function of wavelength over the whole image (upper curve), at position R.A. (J2000) = $23^h 23^{min} 30^s$, Decl. B(J2000) = $58^\circ 50' 25''$ in the bright ring region (curve in the middle), at position R.A. (J2000) = $23^h 23^{min} 26.3^s$, Decl. (J2000) = $58^\circ 51' 21''$ in the northernmost region (lower curve). For the last two curves, the photometry was done over the central pixel and its eight neighbours.

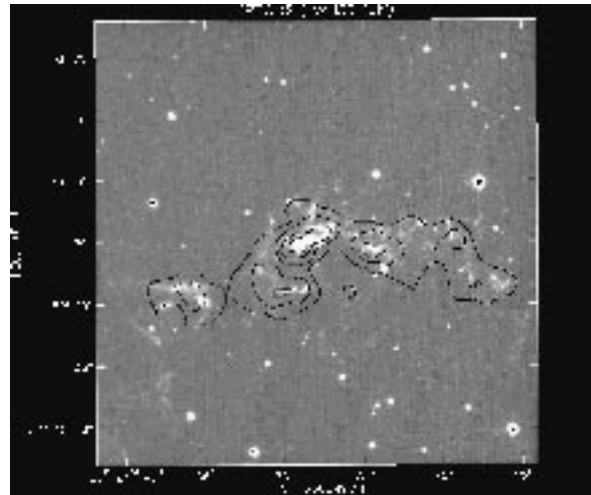


Fig. 4. Correlation between fast moving knots as seen in SII and the SIV knots seen by ISOCAM. To obtain the best correlation, the IR image has been shifted by $10''$; $2''$ are probably due to the movement of the knots since their observations in the visible; the remaining $8''$ are attributed to ISO pointing error. The SII image is courtesy of R. Fesen & R. Downes.

heat the dust through collisions. As can be seen in Fig. 5, the X-ray emission has a much smoother distribution than the dust emission. Thus the excess dust emission seen at the positions of the knots indeed appears to originate from an increase in the amount of dust at the positions of the knots, rather than an enhancement of the heating mechanism.

To determine the dust temperature and mass, we need to know the dust composition and size distribution. Kozasa et al. (1991) have studied dust formation and composition in the context of SN 1987A. They find that dust condenses in the metal rich core at an age of ~ 500 days. Al_2O_3 forms first in most of the oxygen rich region, consuming most of the aluminum, and

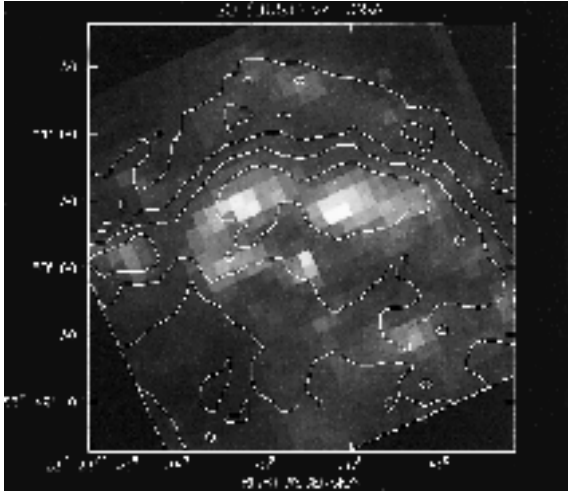


Fig. 5. $11.3\mu\text{m}$ dust emission image of Cas A with overlaid on it the X-ray contour plot from the public ROSAT archive. At each contour the flux is divided by 2. The X-ray image has been shifted within the ROSAT positional uncertainty ($10''$) in order to find the best correlation.

giving a total Al_2O_3 mass of $\sim 0.01 M_\odot$. Next, magnesium-silicate, MgSiO_3 , forms. The total mass of MgSiO_3 could be up to $\sim 0.1 M_\odot$. Kozasa et al. find that the Al_2O_3 grain sizes are $\sim 10\text{\AA}$, while the MgSiO_3 grains are $\sim 70\text{\AA}$. Sputtering of these grains is important in the hot, X-ray emitting gas, and we estimate a life time of $\sim 10^3$ years for the MgSiO_3 grains and a factor of ten less for the Al_2O_3 grains. In the FMK energy spectrum shown in Fig.3, we do see some excess at 9.8 and $11.3\mu\text{m}$ probably related to a silicate feature. It is out of the scope of this paper to perform detailed calculation of dust temperature and mass. The temperature is just estimated by fitting the observed continuum at $12\mu\text{m}$ and in the LW9 filter with a blackbody. The LW9 filter encompasses the NeIII line; but we expect its contribution to be less than 30% of the flux. The temperature of the grains in the evaporating flows, determined that way, is 220K, when the temperature of the dust at the origin of the northernmost faint emission is much lower, 115K. A temperature of 220 K can be reached by grains collisionally heated by the hot electrons in the evaporating gas around FMK's ($n_e \sim 300\text{cm}^{-3}$, $T_e \sim 5.10^6\text{K}$), if their size is less than $\sim 50\text{\AA}$, (Dwek 1986). In the evaporating flows, the dust-gas collision time is of the same order as the dust cooling time, so that the dust is not so far from thermal equilibrium. A dust mass of the order of $10^{-7} M_\odot$ is required to account for the $12\mu\text{m}$ flux observed in the brightest knot; (the distance of Cas A is taken to be equal to 3kpc). This is much less than the typical grain mass expected in a knot, $10^{-4} M_\odot$ (Dwek et al. 1981). But most of the mass is inside the knots in the form of cold grains. At $10\mu\text{m}$ we are only probing those SN condensates which have been heated substantially in the evaporating flows.

Acknowledgements. We thanks R. Fesen and R. Downes for providing us with the SII optical image.

References

- Amari S. et al., 1992, ApJ 337, 494
 Borkowski K.J. et al., 1996, ApJ 466, 866
 Bouchet P., Danziger I. J., Lucy L. B., 1991, AJ 102, 1135
 Braun R., 1987, A&A 171, 233
 Clayton D.D., 1978, Moon and Planets 19, 109
 Chevalier R.A., Kirshner R.P., 1979, ApJ 233, 154
 Colgan S.W.J. et al., 1994, ApJ 427, 874
 Dinerstein H.L. et al., 1987, ApJ 312, 314
 Dwek E., Werner M.W., 1981, ApJ 248, 138
 Dwek E., 1986, ApJ 302, 363
 Dwek E. et al., 1987, ApJ 315, 571
 Fabian A.C. et al., 1980, MNRAS 193, 175
 Fesen R.A., Becker R.H., Goodrich R.W., 1988, ApJ 329, L89
 Kozasa T., Hasegawa H., Nomoto K., 1991, A&A 249, 474
 Lamb S.A., 1978, ApJ 220, 186
 Lucy L.B. et al. 1989, in IAU Colloq. 120, ed. G. Tenorio-Tagle, M. Moles, & J. Melnick (Berlin: Springer-Verlag), 164
 Moseley H. et al., 1989, Nature 340, 697
 Murray S.S. et al., 1979, ApJ 234, L69
 Reed J.E. et al., 1995, ApJ 440, 706
 Starck J.L., Murtagh F., Bijaoui A., 1995, Graphical models and image processing 57, 420
 Suntzeff N.B. et al., 1991, AJ 102, 1118
 van den Bergh S., Kamper K.W., 1983, ApJ 268, 129
 Wooden D.H. et al., 1993, ApJS 88, 477